

Minerva Access is the Institutional Repository of The University of Melbourne

Author/s:

Oshitani, J;Hino, M;Oshiro, S;Mawatari, Y;Tsuji, T;Jiang, Z;Franks, GV

Title:

Conversion air velocity at which reverse density segregation converts to normal density segregation in a vibrated fluidized bed of binary particulate mixtures

Date:

2022-05-01

Citation:

Oshitani, J., Hino, M., Oshiro, S., Mawatari, Y., Tsuji, T., Jiang, Z. & Franks, G. V. (2022). Conversion air velocity at which reverse density segregation converts to normal density segregation in a vibrated fluidized bed of binary particulate mixtures. *Advanced Powder Technology*, 33 (5), <https://doi.org/10.1016/j.appt.2022.103583>.

Persistent Link:

<https://hdl.handle.net/11343/325303>

# **Conversion air velocity at which reverse density segregation converts to normal density segregation in a vibrated fluidized bed of binary particulate mixtures**

Jun Oshitani <sup>a\*</sup>, Masaki Hino <sup>a</sup>, Shinichiro Oshiro <sup>b</sup>, Yoshihide Mawatari <sup>c</sup>,  
Takuya Tsuji <sup>d</sup>, Zhaohua Jiang <sup>d</sup> and George V. Franks <sup>e,f</sup>

<sup>a</sup> *Department of Applied Chemistry, Okayama University of Science, 1-1 Ridai-cho, Kita-ku,  
Okayama 700-0005, Japan*

<sup>b</sup> *Division of Applied Chemistry, Okayama University, 3-1-1 Tsushima-naka, Kita-ku, Okayama  
700-8530, Japan*

<sup>c</sup> *Department of Applied Chemistry, Kyushu Institute of Technology, Sensui 1-1, Tobata, Kitakyushu,  
Fukuoka 804-8550, Japan*

<sup>d</sup> *Department of Mechanical Engineering, Osaka University, 2-1 Yamadaoka Suita, Osaka 565-  
0871, Japan*

<sup>e</sup> *Department of Chemical Engineering, University of Melbourne, Parkville 3010, VIC, Australia*

<sup>f</sup> *ARC Centre of Excellence for Enabling Eco-Efficient Beneficiation of Minerals*

---

\*To whom correspondence may be addressed.

Tel: +81 86 256 9403, E-mail address: oshitani@dac.ous.ac.jp (J. Oshitani)

## **Abstract**

It is well known, when binary mixtures of different-density particles of the same size are vertically vibrated or fluidized by airflow through the bottom, the particles segregate by density. Reverse density segregation occurs in the vibrated bed; heavier particles move upward and lighter ones move downward, and normal density segregation occurs in the fluidized bed; lighter particles move upward and the heavier ones move downward. In this study, we investigated the particles' behavior in a vertically vibrated fluidized bed at various air velocity using two types of particulate mixtures of glass beads (GB) and stainless steel powder (SP) or iron powder (IP) of same size. We found that reverse segregation converts to normal segregation at a certain air velocity; here we call it "conversion air velocity". Then, we investigated the likely origin of the conversion air velocity considering the minimum fluidization air velocity  $u_{mf}$  determined for the three monocomponent particles (GB, SP and IP) with and without vibration. We found that the conversion air velocity is close to the  $u_{mf}$  of the lower density particles (GB) with vibration, indicating that the conversion from reverse segregation to normal segregation occurs around  $u_{mf}$  of lighter particles with vibration.

**Keywords:** Density segregation, Vibrated fluidized bed, Separation

## 1. Introduction

Powder handling is important in various engineering applications, such as mineral processing, food processing, pharmaceutical preparation, surface coating, granulation, and grain drying [1–4]. Addition of fluidizing airflow and/or vibration to the powder bed is a powerful tool to induce segregation of binary particulate mixtures for effective powder handling.

When binary mixtures of different-density particles of the same size are fluidized by airflow through the bottom, normal density segregation occurs; lighter particles move upward and the heavier ones move downward. The fundamentals of the segregation have been widely investigated, and the segregation has been applied to dry gravity separation of particulate mixtures [5–24]. The addition of vibration to the fluidized bed is a useful method to achieve good fluidization of fine cohesive particles [25–32]. The vibration affects the cohesive particles aggregate size, the characteristics of the bed expansion, the pressure drop through the bed and so on. The vibrated fluidized bed is also useful to improve the segregation of non-cohesive binary particulate mixtures [33–43]. Recently, we reported the advantage of the addition of vertical vibration to the fluidized bed [42]. When a fine particulate sand mixture of heavy sand and lighter silica sand was fluidized without the vibration, normal density segregation was not induced because the density difference of the two sands ( $< 1.3 \text{ g/cm}^3$ ) was not large enough. On the other hand, normal density segregation was induced when the sand mixture was fluidized with the vibration. We also found that the highest degree of the density segregation is obtained when the air velocity is close to the minimum fluidization velocity of the sand mixture regardless of the initial bed height, and that the degree of the density segregation surprisingly oscillates with increasing vibration intensity.

The addition of vertical vibration to binary particulate mixtures without airflow has been also widely investigated [44]. As the size segregation, Brazil-nut effect (BN) and reverse Brazil-nut effect (RBN) are famous. BN or RBN is observed when binary mixtures of different-sized particles are vertically vibrated [45–48]. Larger particles move upward for BN or smaller ones move upward for RBN, which depends on the relationship between the size ratio and density ratio of the particles. Li

et al. experimentally and theoretically investigated BN and RBN in the vibrated fluidized bed by changing the air velocity [49]. The authors found that BN converts to RBN upon increasing the air velocity from zero to a critical value, and explained the conversion based on the fundamental theory of dynamics. The conversion air velocity was predicted to be close to  $0.68 \times u_{mf}$  where  $u_{mf}$  is the minimum fluidization air velocity of the binary mixture. However, the origin of the conversion air velocity was not discussed in the literature.

Density segregation in a vibrated bed has been also investigated [50–55]. When binary mixtures of different-density particles of the same size are vertically vibrated, reverse density segregation occurs at smaller frequency of vibration; heavier particles move upward and lighter ones move downward. The sandwich type segregation occurs at larger frequency; a layer of heavier particles is sandwiched between an upper layer and a lower layer of lighter particles. The existence of interstitial air in the powder bed is deemed responsible for the phenomena because these segregations do not occur under vacuum conditions. Zeilstra et al. showed the mechanisms of these segregations considering the difference in acceleration from the air drag and the difference in inertial mass in collisions [54, 55].

As above, reverse density segregation and normal density segregation are generally characteristics of the vibrated bed and the fluidized bed, respectively. It is expected that reverse segregation would convert to the normal segregation at a certain air velocity in a vibrated bed if the air velocity is increased from zero. However, the investigation of the conversion from reverse segregation to normal segregation for density segregation has not been carried out while that for the size segregation has been conducted by Li et al. [49]. In this study, we investigated the conversion using two types of binary mixtures of different-density particles of the same size, and we also investigated the origin of the conversion air velocity considering minimum fluidization air velocity of the lighter and heavier particles with and without vibration. Better understanding of the conversion velocity will enable determining the correct operating conditions to effect efficient separations.

## 2. Experimental

### 2.1. Particulate mixture

Two types of particulate mixtures A and B of 50%:50% bulk volume fraction are used. Mixture A consists of glass beads (GB1, bulk density 1.5 g/cm<sup>3</sup>) and stainless steel powder (SP, bulk density 4.0 g/cm<sup>3</sup>); the GB and SP are non-cohesive spherical particles of 0.21–0.25 mm diameter. Mixture B consists of glass beads (GB2, bulk density 1.5 g/cm<sup>3</sup>) and iron powder (IP, bulk density 4.4 g/cm<sup>3</sup>); the GB and IP are non-cohesive spherical particles of 0.15–0.18 mm diameter. The particle properties are shown in Table 1 including the density of the bulk form of the powdered materials which are typically; glass (2.2 to 2.5 g/cm<sup>3</sup>), stainless steel (7.5 to 8.0 g/cm<sup>3</sup>) and iron (7.9 g/cm<sup>3</sup>).

### 2.2. Vibrated fluidized bed and measurement of air velocity versus pressure drop

The apparatus used previously [42] was used in this study. The apparatus consists of a cylindrical column of inner diameter = 100 mm, an air distributor with a textile felt held between two perforated metal plates and an air chamber. The vertical vibration was generated by two vibration motors connected to the side of the air chamber. The amplitude  $A$  was varied by tuning unbalanced weights in the vibration motors. The frequency  $f$  was controlled using an inverter. The ratio of vibration acceleration to gravitational acceleration  $g$ , so-called vibration intensity  $\Gamma (= A(2\pi f)^2/g)$ , was used as an index of the vibration strength. The  $A$ ,  $f$  and  $\Gamma$  for the experiments using Mixture A and Mixture B are shown in Table 2. There are two dimensionless parameters for characterizing the vibration strength;  $\Gamma$  for “mild fluidization” and  $S (= A^2(2\pi f)^2/gd)$  for “strong fluidization” where  $d$  is the particle diameter [56]. The choice of the parameter depends on whether the powder bed follows the motion of the bottom of the container in *mild* fluidization or not in *strong* fluidization. We employed  $\Gamma$  in order to investigate the density segregation in *mild* fluidization using relatively small amplitude and frequency in this study. The vibration intensity  $\Gamma$  was chosen somewhat arbitrarily as 4.4 for Mixture A and 3.4 for Mixture B as these values were found to produce good reverse segregation when only vibration was applied to the bed.

The monocomponent particles of GB, SP or IP was put into the cylindrical column to a bed height = 50 mm. Air from a compressor was injected into the particles through the air distributor. The superficial air velocity  $u_0$  was varied by an airflow controller. For the determination of minimum fluidization air velocity  $u_{mf}$ , the superficial air velocity was gradually increased from zero with and without the vertical vibration, and the pressure drop across the particles  $\Delta P$  was measured by a manometer. Graphs of  $u_0$  versus  $\Delta P$  with and without vibration were made to determine  $u_{mf}$  as described elsewhere [57]. The point of intersection of a linearly increasing line for the fixed powder bed and a flat line for the fluidized powder bed was regarded as  $u_{mf}$ . The measurements were carried out three times and averaged.

### 2.3. Density segregation experiments

The binary particulate mixture was put into the cylindrical column to a bed height = 100 mm, and was fluidized for 10 min with the vertical vibration at a given air velocity  $u_0$  in the range of 0 ~ 28.6 cm/s for Mixture A and in the range of  $u_0 = 0 \sim 13.2$  cm/s for Mixture B. After the fluidization and the vibration, 10 layers of the particles of approximately 10 mm in height were collected as follows. A ruler is put on the outer wall of the cylindrical column. Each layer of the particles was collected using a vacuum cleaner while watching the ruler at the side of the column. The weight and bulk volume of each layer were measured using an electronic balance and a measuring cylinder, respectively. The particles bulk density  $\rho$  at each layer was calculated by dividing the weight by the bulk volume. As the preliminary experiments, we measured the bulk density of Mixture A and Mixture B for the given bulk volume fractions of SP and IP (see Fig. S1 of the Supplementary material). The bulk density linearly increases with the bulk volume fraction. The equations given by the fitted straight line in the figure were used to estimate the bulk volume fraction of SP ( $V_{SP}$ ) for Mixture A and of IP ( $V_{IP}$ ) for Mixture B at each layer. The estimation gave  $V_{SP}$  and  $V_{IP}$  of 10 layers at the given air velocity with vibration. It should be noted that the bed height during the fluidization and the vibration varies with changing  $u_0$ . However, we confirmed that the bed height returns to be the

initial bed height = 100 mm after the fluidization and the vibration ceased, which might be because non-cohesive spherical particles of same size are used in this study. Therefore, the above-mentioned simple method is reliable to estimate the bulk volume fraction as a function of height through the bed. The segregation efficiency  $E$  was calculated using Eq.(1) to evaluate the degree of segregation, where  $L = 1$  is for the top layer,  $L = 10$  is for the bottom layer, and  $V_{SP\ or\ IP}(L)$  is expressed as a percentage. For a well-mixed non-segregated mixture,  $V_{SP\ or\ IP}(L) = 50\%$  for all layers and thus Eq. (1) gives  $E = 0\%$ . For a perfect normal segregation, lower five layers are SP or IP and thus Eq. (1) gives  $E = 100\%$ . On the other hand, for a perfect reverse segregation, upper five layers are SP or IP and thus Eq. (1) gives  $E = -100\%$ . The experiments were carried out 2 or 3 times for each experimental condition and the results were averaged.

$$E = \frac{1}{10} \left\{ \sum_{L=1}^5 \frac{50 - V_{SP\ or\ IP}(L)}{50} + \sum_{L=6}^{10} \frac{V_{SP\ or\ IP}(L) - 50}{50} \right\} \times 100 \% \quad (1)$$

### 3. Results and discussion

#### 3.1. Reverse segregation and normal segregation

Fig. 1 shows the bulk volume fraction of SP ( $V_{SP}$ ) of each layer and Fig. 2 shows photos of the side views of the powder bed at various air velocities  $u_0$  for Mixture A (0.21–0.25 mm diameter). The photos were taken from video recordings (available in the Supplementary material as “Supplementary video 1”) The video clips of the particles’ behavior at various air velocities  $u_0$  for Mixture A were recorded over a period of 10 mins but played back at 20 times speed up. The dark color and light color in the photos show stainless steel powder (SP) and glass beads (GB), respectively.  $V_{SP}$  of upper layers is close to 100% and  $V_{SP}$  of lower layers is close to 0% at  $u_0 = 0$  and 2.2 cm/s, indicating that reverse segregation occurs when only vibration and lower air velocity is applied. The reverse segregation can be observed in the photos; although it is not easy to see due to the low color contrast, the upper area is darker than the lower area. It is observed by the video recordings that the downward convection of the particles exists near the side wall, and the GB moving downward accumulate at the

bottom. On the other hand,  $V_{SP}$  of upper layers is close to 0% and  $V_{SP}$  of lower layers is close to 100% at  $u_0 = 8.8 \sim 19.8$  cm/s, indicating that normal segregation occurs at these air velocity ranges. The normal segregation is clearly shown by the photos and the video recordings.  $V_{SP}$  of layer 1 ~ 7 at  $u_0 = 24.2$  cm/s and of layer 1 ~ 9 at  $u_0 = 28.6$  cm/s are close to 50%, indicating that GB and SP tend to mix at too high air velocity due to violent bubbling as shown by the photos and the video recordings.

Here we focused on the fact that reverse segregation converts to normal segregation between  $u_0 = 2.2$  and 8.8 cm/s for Mixture A, and next we investigated the conversion using the other particulate Mixture B (0.15–0.18 mm diameter). Fig. 3 shows the bulk volume fraction of IP ( $V_{IP}$ ) of each layer at various air velocities  $u_0$  for Mixture B. As with the case of Mixture A, reverse segregation occurs at  $u_0 = 0$  and 1.0 cm/s, and normal segregation occurs at  $u_0 = 4.1$  and 7.1 cm/s. The reverse segregation converts to normal segregation between  $u_0 = 1.0$  and 4.1 cm/s. Here we varied  $u_0$  in smaller increments around the conversion. The result obtained at  $u_0 = 1.5$  cm/s is interesting.  $V_{IP}$  of layer 1 is close to 0%; the top layer consists of GB. As the layer goes down,  $V_{IP}$  increases from approx. 0% at layer 1 to approx. 100% at layer 3, whereas  $V_{IP}$  decreases to approx. 30% at layer 5. Again,  $V_{IP}$  increases to approx. 65% at layer 8, whereas  $V_{IP}$  slightly decreases to approx. 55% at layer 10. It seems to that the reverse segregation is reduced and the normal segregation is induced to a certain extent at  $u_0 = 1.5$  cm/s, because IP cannot move up to the top layer and almost half of the IP stays in the lower five layers. The normal segregation is induced to a greater extent at  $u_0 = 2.0$  cm/s.  $V_{IP}$  of layer 1~3 is close to 0%; the top three layers consist of GB.  $V_{IP}$  of the lower five layers is larger compared to that at  $u_0 = 1.5$  cm/s. However, surprisingly,  $V_{IP}$  clearly decreases from approx. 100% at layer 6 to approx. 50% at layer 10. It seems that the IP at middle height layers cannot move downward across the GB-rich layers.

### 3.2. Conversion air velocity

The above results clarified that the reverse segregation converts to the normal segregation at a certain critical air velocity, that is, the conversion air velocity. In order to investigate the origin of the

conversion air velocity, the minimum fluidization air velocity  $u_{mf}$  was determined from plots of air velocity  $u_0$  versus pressure drop  $\Delta P$ . Fig. 4 and 5 show  $\Delta P$  as a function of  $u_0$  for the particles used to prepare Mixture A and B. The dotted lines in the figures are  $u_{mf}$  for GB, SP and IP with and without vibration.  $u_{mf}$  and  $\Delta P$  at  $u_0 \geq u_{mf}$  of the lighter particles (GB) is less than those of heavier particle (SP and IP), which is a well known characteristic of fluidized beds.  $u_{mf}$  with vibration is less than that without vibration, whereas  $\Delta P$  with vibration is larger than that without vibration for all of GB, SP and IP. Similar tendency was reported previously [25, 28]. The decrease in powder bed voidage due to consolidation with vibration is related to the decrease in  $u_{mf}$  and the increase in  $\Delta P$ .

Fig. 6 and 7 show the segregation efficiency  $E$  as a function of  $u_0$  for Mixture A and B, respectively. The graphs clearly show the transition of the particles' behavior;  $E \approx -75\%$  at lower  $u_0$  means the reverse segregation,  $E \approx 90\%$  at middle ranged  $u_0$  means the normal segregation, and  $E \approx 0\%$  at higher  $u_0$  means mixing. The conversion air velocity is around 3.5 cm/s for Mixture A and around 1.5 cm/s for Mixture B. The dotted lines in the figures are the  $u_{mf}$  of GB, SP and IP with and without vibration. It is found that the  $u_{mf}$  of the GB is closely related to the conversion air velocity. Especially, the  $u_{mf}$  of the GB "with vibration" is close to the conversion air velocity. The results indicate that the reverse segregation converts to the normal segregation near at the minimum fluidization air velocity of lighter particles with vibration.

Hereafter, we discuss the possible mechanism why the conversion from the reverse segregation to the normal segregation occurs around the  $u_{mf}$  of lighter particles with vibration. Zeilstra et al. showed the mechanism of the reverse segregation as follows [54, 55]. The vertical vibration (without fluidization) induces the cyclic compaction and decompaction of the powder bed with the oscillating gas flow in the powder bed. Air drag is generated due to the pumping of air in combination with the cyclic compaction and decompaction. The difference in acceleration from the air drag causes the heavier particles to move upward, resulting in the reverse segregation [54, 55]. Then, we consider the possible mechanism as follows. If the air is vertically injected into the vibrated powder bed through the bottom and the air velocity reaches the  $u_{mf}$  of lighter particles with vibration, the lighter particles

begin to be fluidized. The air pumping effect (due to compaction and decompaction) is weakened and the difference in acceleration from the air drag becomes negligible. As the result, the reverse segregation does not occur. Above the  $u_{mf}$ , even though the binary mixture is vertically vibrated, the heavier particles sink in the fluidized bed of the lighter particles based on density difference resulting in normal segregation. In short, the fluidization of the lighter particles induced by the airflow through the bottom suppresses the effect of vertical vibration that would otherwise induce reverse segregation.

#### **4. Conclusion**

We investigated density segregation in a vibrated fluidized bed with increasing air velocity from zero. Two types of binary mixtures of same-sized different-density particles were used for the experiments. We found that the reverse segregation occurs when only vibration or lower air velocity is applied, and that normal segregation occurs at middle range of air velocity. At very high air velocities mixing occurs. These results indicate that reverse segregation converts to the normal segregation at a certain critical air velocity, that is, the conversion air velocity. In order to investigate the origin of the conversion air velocity, we determined the minimum fluidization air velocity  $u_{mf}$  of the lighter particles and the heavier particles with and without vibration. We found that the  $u_{mf}$  of the lighter particles with vibration is close to the conversion air velocity, indicating that the conversion from reverse segregation to normal segregation occurs around the  $u_{mf}$  of the lighter particles. As the possible mechanism, we suggest that the fluidization of the lighter particles induced by the airflow through the bottom suppresses the effect of vertical vibration to induce reverse segregation.

#### **Acknowledgements**

This work was supported in part by JSPS KAKENHI Grant Number JP18H03406 and the Information Center of Particle Technology to Jun Oshitani. George Franks acknowledges funding support from the Australian Research Council for the ARC Centre of Excellence for Enabling Eco-Efficient Beneficiation of Minerals, grant number CE200100009.

## References

- [1] K. Higashitani, H. Makino, S. Matsusaka, Powder technology handbook, fourth ed., CRC Press, 2019.
- [2] H.Y. Wang, A. Mustaffar, A.N. Phan, V. Zivkovic, D. Reay, R. Law, K. Boodhoo, A review of process intensification applied to solids handling, *Chem. Eng. Process. Process Intensif.*, 118 (2017) 78–107.
- [3] I. Hafsa, S. Mandato, T. Ruiz, P. Schuck, R. Jeantet, S. Mejean, S. Chevallier, B. Cuq, Impact of the agglomeration process on structure and functional properties of the agglomerates based on the durum wheat semolina, *J. Food Eng.*, 145 (2015) 25–36.
- [4] F.J. Muzzio, T. Shinbrot, B.J. Glasser, Powder technology in the pharmaceutical industry: the need to catch up fast, *Powder Technol.*, 124 (2002) 1–7.
- [5] P.N. Rowe, A.W. Nienow, Particle mixing and segregation in gas fluidized beds: a review, *Powder Technol.* 15 (1976) 141–147.
- [6] W.C. Yang, D.L. Kealrns, Rate of particle separation in a gas fluidized bed, *Ind. Eng. Chem. Fundam.* 21 (1982) 228–235.
- [7] A.C. Hoffmann, L.P.B.M. Janssen, J. Prins, Particle segregation in fluidized binary mixture, *Chem. Eng. Sci.* 48 (1993) 1583–1592.
- [8] A. Marzocchella, P. Salatino, V.D. Pastena, L. Lirer, Transient fluidization and segregation of binary mixture of particles, *AIChE J.* 46 (2000) 2175–2182.
- [9] G.A. Bokkers, M. van Sint Annaland, J.A.M. Kuipers, Mixing and segregation in a bidisperse gas–solid fluidised bed: a numerical and experimental study, *Powder Technol.* 140 (2004) 176–186.
- [10] G. Olivieri, A. Marzocchella, P. Salatino, Segregation of fluidized binary mixtures of granular solids, *AIChE J.* 50 (2004) 3095–3106.
- [11] K.P. Galvin, R. Swann, W.F. Ramirez, Segregation and dispersion of a binary system of particles

in a fluidized bed, *AIChE J.* 52 (2006) 3410.

- [12] G.G. Joseph, J. Leboireiro, C.M. Hrenya, A.R. Stevens, Experimental segregation profiles in bubbling gas-fluidized beds, *AIChE J.* 53 (2007) 2804–2813.
- [13] X. Wang, N.J. Miles, S. Kingman, Segregation of ultrafine particles in a centrifugal fluidized bed separator, *Adv. Powder Technol.* 19 (2008) 335–348.
- [14] B. Formisani, R. Girimonte, T. Longo, The fluidization pattern of density-segregating binary mixtures, *Chem. Eng. Res. Des.* 86 (2008) 344–348.
- [15] A. Rao, J.S. Curtis, B.C. Hancock, C. Wassgren, Classifying the fluidization and segregation behavior of binary mixtures using particle size and density ratios, *AIChE J.* 57 (2011) 1446–1458.
- [16] Y. Zhang, W. Zhong, B. Jin, R. Xiao, Mixing and segregation behavior in a spoutfluid bed: Effect of the particle density, *Ind. Eng. Chem. Res.* 52 (2013) 5489–5497.
- [17] J. Oshitani, M. Ohnishi, M. Yoshida, G.V. Franks, Y. Kubo, S. Nakatsukasa, Dry separation of particulate iron ore using density-segregation in a gas-solid fluidized bed, *Adv. Powder Technol.* 24 (2013) 554–559.
- [18] Q. Wang, W. Yin, B. Zhao, H. Yang, J. Lu, L. Wei, The segregation behaviors of fine coal particles in a coal beneficiation fluidized bed, *Fuel Process Technol.* 124 (2014) 28–34.
- [19] S.L.L. Seah, E.W.C. Lim, Density segregation of dry and wet granular mixtures in gas fluidized beds, *AIChE J.* 61 (2015) 4069–4086.
- [20] J. Oshitani, K. Teramoto, M. Yoshida, Y. Kubo, S. Nakatsukasa, G.V. Franks, Dry beneficiation of fine coal using density-segregation in a gas-solid fluidized bed, *Adv. Powder Technol.* 27 (2016) 1689–1693.
- [21] J. Huang, Y. Lu, H. Wang, A new quantitative measurement method for mixing and segregation of binary-mixture fluidized bed by capacitance probe, *Chem. Eng. J.* 99–108 (2017).
- [22] J. He, C. Liu, J. Xie, P. Hong, Y. Yao, Beneficiation of coarse particulate iron ore by using a dry density-based fluidized bed separator, *Powder Technol.* 319 (2017) 346–355.

- [23] R. Girimonte, B. Formisani, V. Vivacqua, The relationship between fluidization velocity and segregation in two-component gas fluidized beds: Density- or size-segregating mixtures, *Chem. Eng. J.* 335 (2018) 63–73.
- [24] J. Oshitani, S. Hayashi, D.Y.C. Chan, Order from Chaos: Dynamics of density segregation in continuously aerated granular systems, *Adv. Powder Technol.* 31 (2020) 843–847
- [25] E. Marring, A.C. Hoffmann, L.P.B.M. Janssen, The effect of vibration on the fluidization behaviour of some cohesive powders, *Powder Technol.* 79 (1994) 1–10.
- [26] S.M. Tasirin, N. Anuar, Fluidization behavior of vibrated and aerated beds of starch powders, *J. Chem. Eng. Jpn.* 34 (2001) 1251–1258.
- [27] Y. Mawatari, M. Tsunekawa, Y. Tatemoto, K. Noda, Favorable vibrated fluidization conditions for cohesive fine particles, *Powder Technology* 154 (2005) 54–60.
- [28] C. Xu, J. Zhu, Parametric study of fine particle fluidization under mechanical vibration, *Powder Technol.* 161 (2006) 135–144.
- [29] J.M. Valverde, A. Castellanos, Effect of vibration on agglomerate particulate fluidization, *AIChE J.* 52 (2006) 1705–1714.
- [30] D. Barletta, M. Poletto, Aggregation phenomena in fluidization of cohesive powders assisted by mechanical vibrations, *Powder Technol.* 225 (2012) 93–100.
- [31] D. Barletta, P. Russo, M. Poletto, Dynamic response of a vibrated fluidized bed of fine and cohesive powders, *Powder Technol.*, 237 (2013) 276–285.
- [32] Y. Mawatari, Y. Hamada, M. Yamamura, H. Kage Flow pattern transition of fine cohesive powders in a gas-solid fluidized bed under mechanical vibrating conditions, *Procedia Eng.* 102 (2015) 945–951.
- [33] X. Yang, Y. Zhao, Z. Luo, S. Song, C. Duan, L. Dong, Fine coal dry cleaning using a vibrated gas-fluidized bed, *Fuel Process. Technol.* 106 (2013) 338–343.
- [34] C.R.K. Windows-Yule, N. Rivas, D.J. Parker, A.R. Thornton, Low-frequency oscillations and convective phenomena in a density-inverted vibrofluidized granular system, *Phys. Rev. E* 90

(2014) 062205.

- [35] L. Sun, F. Zhao, Q. Zhang, D. Li, H. Lu, Numerical simulation of particle segregation in vibration fluidized beds, *Chem. Eng. Technol.* 37 (2014) 2109–2115.
- [36] P. Zhao, Y. Zhao, Z. Chen, Z. Luo, Dry cleaning of fine lignite in a vibrated gasfluidized bed: segregation characteristics, *Fuel* 142 (2015) 274–282.
- [37] X. Yang, Z. Fu, J. Zhao, E. Zhou, Y. Zhao, Process analysis of fine coal preparation using a vibrated gas-fluidized bed, *Powder Technol.*, 279 (2015) 18–23.
- [38] J. He, Y. Zhao, J. Zhao, Z. Luo, C. Duan, Y. He, Enhancing fluidization stability and improving separation performance of fine lignite with vibrated gas-solid fluidized bed, *Can. J. Chem. Eng.*, 93 (2015) 1793–1801.
- [39] L. Dong, Y. Zhang, Y. Zhao, L. Peng, E. Zhou, L. Cai, B. Zhang, C. Duan, Effect of active pulsing air flow on gas-vibro fluidized bed for fine coal separation, *Adv. Powder Technol.* 27 (2016) 2257–2264.
- [40] E. Cano-Pleite, F. Hernández-Jiménez, A. Acosta-Iborra, T. Tsuji, C.R. Müller, Segregation of equal-sized particles of different densities in a vertically vibrated fluidized bed, *Powder Technol.* 316 (2017) 101–110.
- [41] D. Su, Z. Luo, L. Lei, Y. Zhao, Segregation modes, characteristics, and mechanisms of multi-component lignite in a vibrated gas-fluidized bed, *Int. J. Min. Sci. Technol.* 28 (2018) 251–258.
- [42] J. Oshitani, R. Sugo, Y. Mawatari, T. Tsuji, Z. Jiang, G.V. Franks, Dry separation of fine particulate sand mixture based on density-segregation in a vibro-fluidized bed, *Adv. Powder Technol.* 31 (2020) 4082–4088.
- [43] Z. Jiang, K. Rai, T. Tsuji, K. Washino, T. Tanaka, J. Oshitani, Upscaled DEM-CFD model for vibrated fluidized bed based on particle-scale similarities, *Adv. Powder Technol.* 31 (2020) 4598–4618.
- [44] A.D. Rosato, K. Windows-Yule, *Segregation in vibrated granular systems*, Academic Press, 2020.

- [45] M.E. Möbius, B.E. Lauderdale, S.R. Nagel, H.M. Jaeger, Size separation of granular particles, *Nature* 414 (2001) 270.
- [46] D.C. Hong, P.V. Quinn, S. Luding, Reverse Brazil nut problem: Competition between percolation and condensation, *Phys. Rev. Lett.* 86(2001) 3423–3426.
- [47] A.P.J. Breu, H.-M. Ensner, C.A. Kruelle, I. Rehberg, Reversing the Brazil-nut effect: Competition between percolation and condensation, *Phys. Rev. Lett.* 90 (2003) 014302.
- [48] T. Shinbrot, The Brazil nut effect—in reverse, *Nature* (2004) 352–353.
- [49] L.Li, P.Wu, R.Abdul, L.Wang, S.Zhang, Z.-A. Xie, Energy-dissipation correlated size separation of granular matter under coupling vibration and airflow, *Powder Technol.* 307 (2017) 84–89.
- [50] N. Burtally, P.J. King, M.R. Swift, Spontaneous air-driven separation in vertically vibrated fine granular mixtures, *Science* 295 (2002) 1877–1879.
- [51] N. Burtally, P.J. King, M.R. Swift, M. Leaper, Dynamical behaviour of fine granular glass/bronze mixtures under vertical vibration, *Granular Matter* 5 (2003) 57–66
- [52] P. Biswas, P. Sánchez, M.R. Swift, P.J. King, Numerical simulations of air-driven granular separation, *Phys. Rev. E* 68 (2003) 050301.
- [53] M. Klein, L.L. Tsai, M.S. Rosen, T. Pavlin, D. Candela, R.L. Walsworth, Interstitial gas and density segregation of vertically vibrated granular media, *Phys. Rev. E* 74 (2006) 010301.
- [54] C. Zeilstra, M.A. van der Hoef, J.A.M. Kuipers, Simulation study of air-induced segregation of equal-sized bronze and glass particles, *Phys. Rev. E* 74 (2006) 010302.
- [55] C. Zeilstra, M.A. van der Hoef, J.A.M. Kuipers, Simulation of density segregation in vibrated beds, *Phys. Rev. E* 77 (2008) 031309.
- [56] P. Eshuis, K. van der Weele, D. van der Meer, R. Bos, D. Lohse, Phase diagram of vertically shaken granular matter, *Phys. Fluids*, 19 (2007), 123301.
- [57] J.F. Davidson, R. Clift, D. Harrison, *Fluidization*, second ed., Academic Press, London, 1985.

## Figure Captions

- Figure 1 Bulk volume fraction of SP ( $V_{SP}$ ) in each layer at various air velocities  $u_0$  for Mixture A (0.21–0.25 mm diameter). The vibration intensity was  $\Gamma = 4.4$ . Layer 1 is the top and layer 10 is the bottom.
- Figure 2 Photos of the side views of the powder bed at various air velocities  $u_0$  for Mixture A. 10 minutes after fluidization and vibration are started.
- Figure 3 Bulk volume fraction of IP ( $V_{IP}$ ) in each layer at various air velocities  $u_0$  for Mixture B (0.15–0.18 mm diameter). The vibration intensity was  $\Gamma = 3.4$ . Layer 1 is the top and layer 10 is the bottom.
- Figure 4 Pressure drop  $\Delta P$  as a function of superficial air velocity  $u_0$  for increasing  $u_0$  with and without vibration for the particles used to prepare Mixture A. The dotted lines indicate  $u_{mf}$  for each type of particle with and without vibration. The vibration intensity was  $\Gamma = 4.4$ .
- Figure 5 Pressure drop  $\Delta P$  as a function of superficial air velocity  $u_0$  for increasing  $u_0$  with and without vibration for the particles used to prepare Mixture B. The dotted lines indicate  $u_{mf}$  for each type of particle with and without vibration. The vibration intensity was  $\Gamma = 3.4$ .
- Figure 6 Segregation efficiency  $E$  as a function of superficial air velocities  $u_0$  for Mixture A. The dotted lines indicate  $u_{mf}$  for each type of particle with and without vibration. The vibration intensity was  $\Gamma = 4.4$ .
- Figure 7 Segregation efficiency  $E$  as a function of superficial air velocities  $u_0$  for Mixture B. The dotted lines indicate  $u_{mf}$  for each type of particle with and without vibration. The vibration intensity was  $\Gamma = 3.4$ .

Table 1. Properties of the powders.

	Bulk Density [g/cm <sup>3</sup> ]	Particle size [mm]	Particle density [g/cm <sup>3</sup> ]
Glass Beads GB1	1.5	0.21–0.25	2.2-2.5
Glass Beads GB2	1.5	0.15–0.18	2.2-2.5
Stainless Steel Powder SP	4.0	0.21–0.25	7.5-8.0
Iron Powder IP	4.4	0.15–0.18	7.9

Table 2 The  $A$ ,  $f$  and  $\Gamma$  for the experiments using Mixture A and Mixture B.

	Amplitude $A$ [m]	Frequency $f$ [-]	Vibration intensity $\Gamma$ [-]
Mixture A GB1 & SP	$1.20 \times 10^{-3}$	30	4.4
Mixture B GB2 & IP	$0.93 \times 10^{-3}$	30	3.4

## Supplementary material

### Conversion air velocity at which reverse density segregation converts to normal density segregation in a vibrated fluidized bed of binary particulate mixtures

Jun Oshitani <sup>a\*</sup>, Masaki Hino <sup>a</sup>, Shinichiro Oshiro <sup>b</sup>, Yoshihide Mawatari <sup>c</sup>,  
Takuya Tsuji <sup>d</sup>, Zhaohua Jiang <sup>d</sup> and George V. Franks <sup>e,f</sup>

<sup>a</sup> Department of Applied Chemistry, Okayama University of Science, 1-1 Ridai-cho, Kita-ku, Okayama 700-0005, Japan

<sup>b</sup> Division of Applied Chemistry, Okayama University, 3-1-1 Tsushima-naka, Kita-ku, Okayama 700-8530, Japan

<sup>c</sup> Department of Applied Chemistry, Kyushu Institute of Technology, Sensui 1-1, Tobata, Kitakyushu, Fukuoka 804-8550,  
Japan

<sup>d</sup> Department of Mechanical Engineering, Osaka University, 2-1 Yamadaoka Suita, Osaka 565-0871, Japan

<sup>e</sup> Department of Chemical Engineering, University of Melbourne, Parkville 3010, VIC, Australia

<sup>f</sup> ARC Centre of Excellence for Enabling Eco-Efficient Beneficiation of Minerals

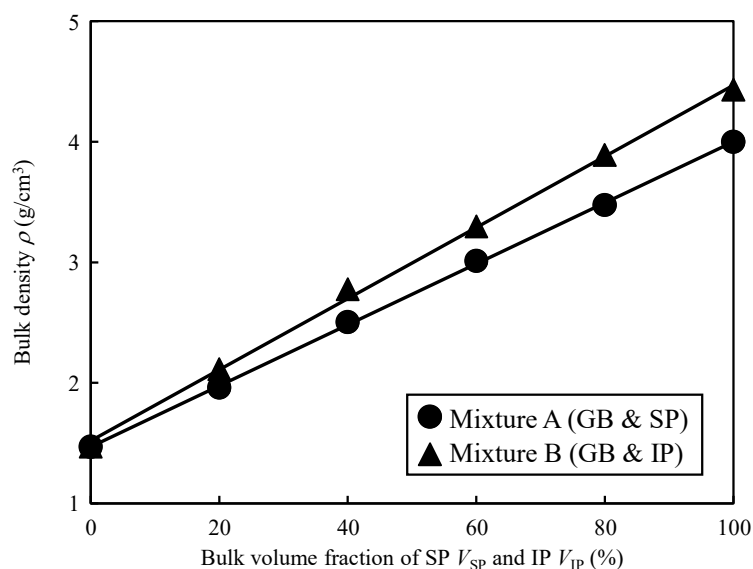


**Fig. S1.** Bulk density as a function of bulk volume fraction of stainless steel powder (SP) for Mixture A and of iron powder (IP) for Mixture B. The straight lines are the best fit to  $\rho$  versus  $V_{SP}$  and  $\rho$  versus  $V_{IP}$ .

#### Supplementary Video Legends

Video clips of the particles' behavior in a vibrated fluidized bed at various air velocities  $u_0$  with the vertical vibration for Mixture A of GB and SP (0.21–0.25 mm diameter), over a period of 10 mins played back at 20 time speed up.

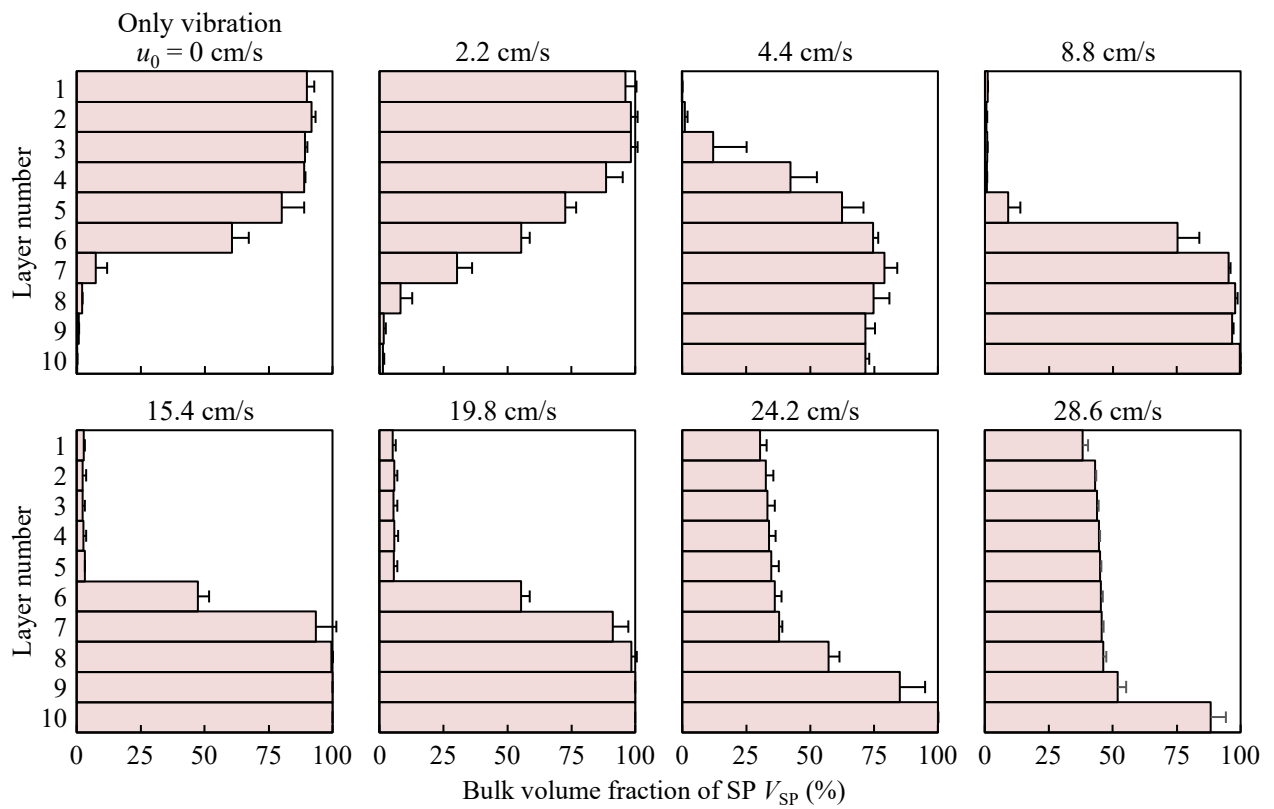


**Fig. 1** Bulk volume fraction of SP  $V_{SP}$  in each layer at various air velocities  $u_0$  for Mixture A.

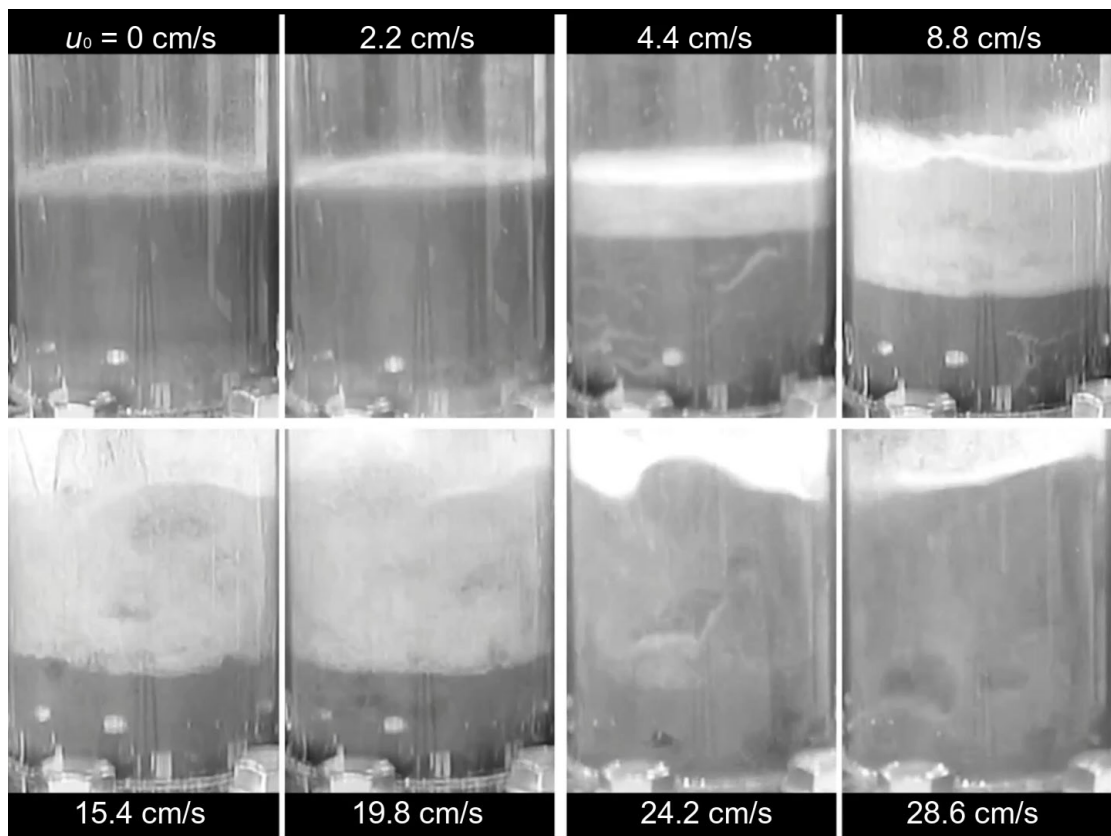


**Fig. 2.** Photos of the side views of the powder bed at various air velocities  $u_0$  for Mixture A. 10 minutes after fluidization and vibration are started.

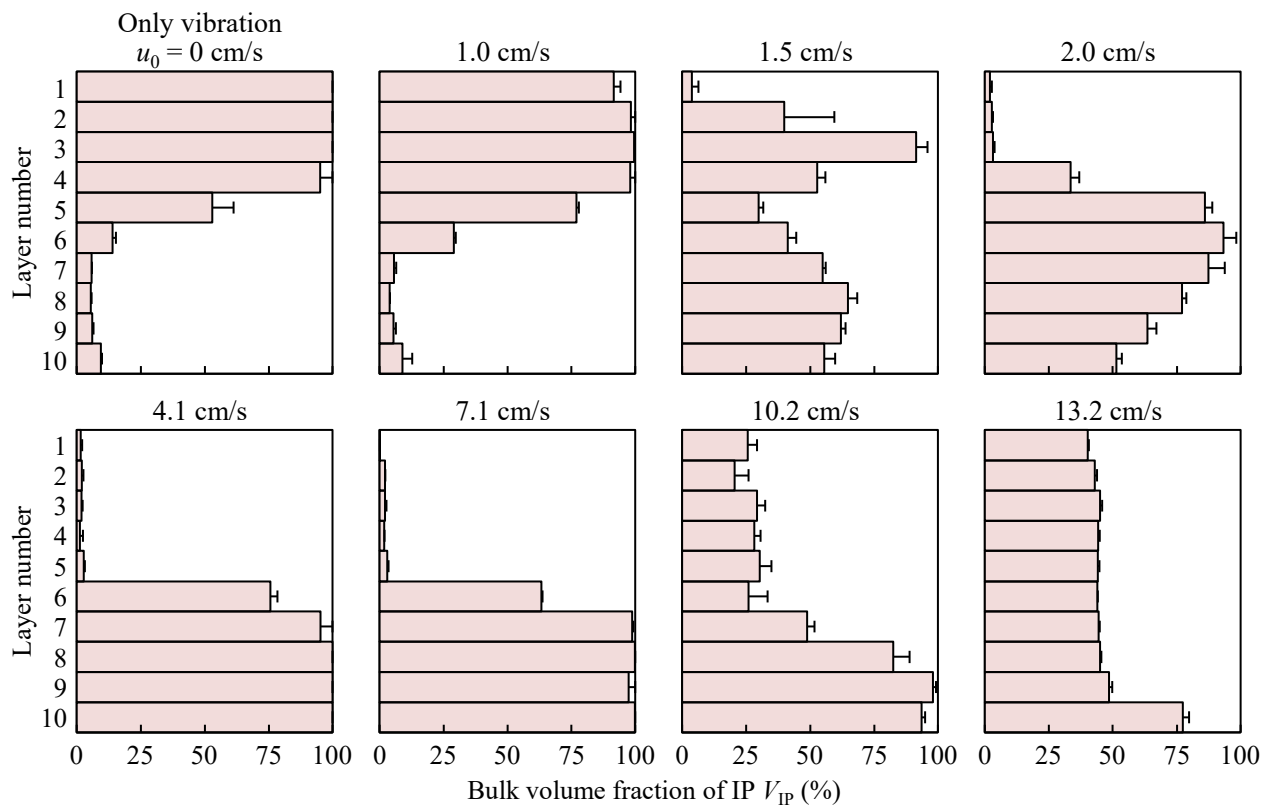


**Fig. 3.** Bulk volume fraction of IP  $V_{IP}$  in each layer at various air velocities  $u_0$  for Mixture B.

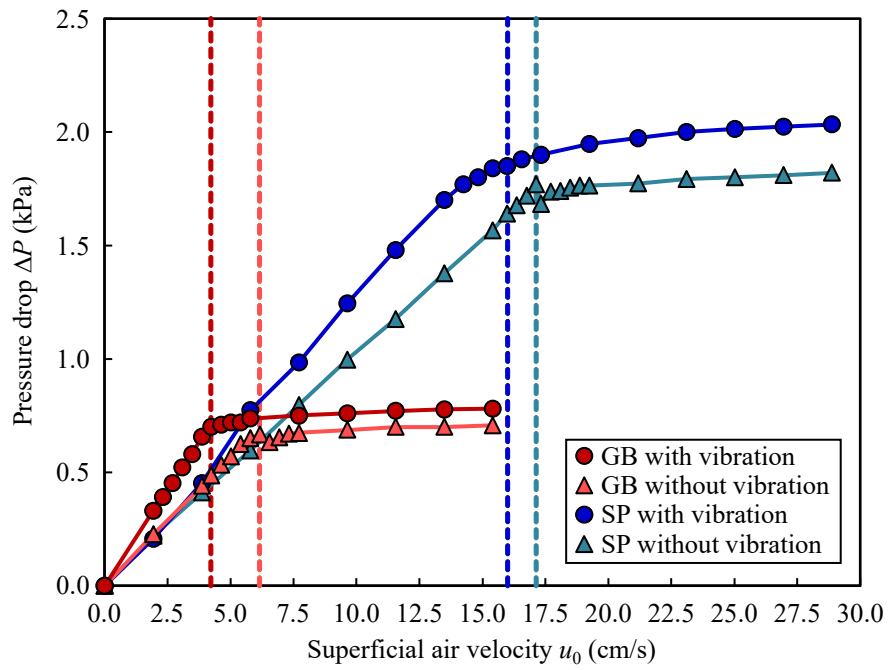


**Fig. 4.** Pressure drop  $\Delta P$  as a function of superficial air velocity  $u_0$  for increasing  $u_0$  with and without vibration for the particles used to prepare Mixture A. Dotted lines are  $u_{mf}$ .

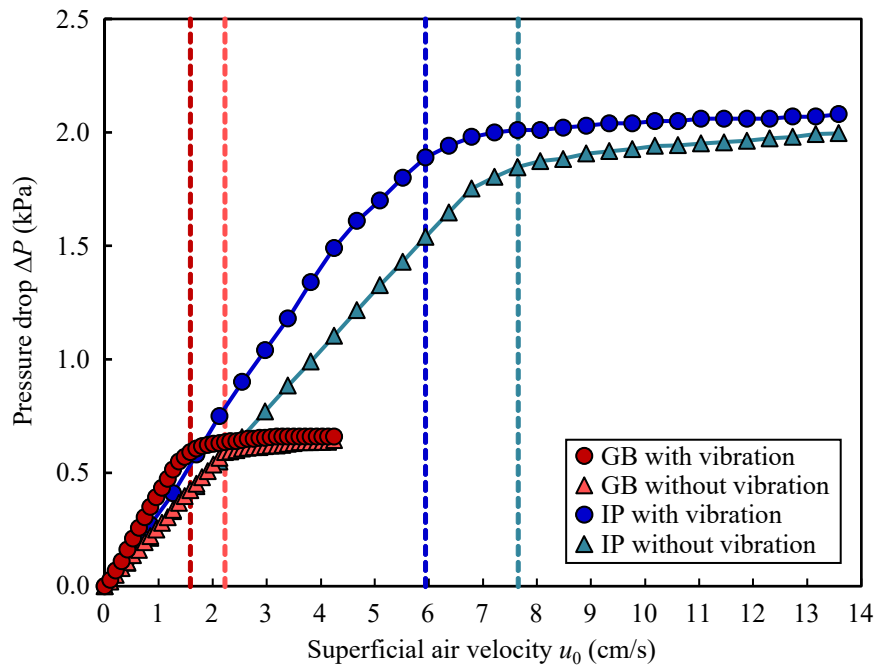


**Fig. 5.** Pressure drop  $\Delta P$  as a function of superficial air velocity  $u_0$  for increasing  $u_0$  with and without vibration for the particles used to prepare Mixture B. Dotted lines are  $u_{mf}$ .

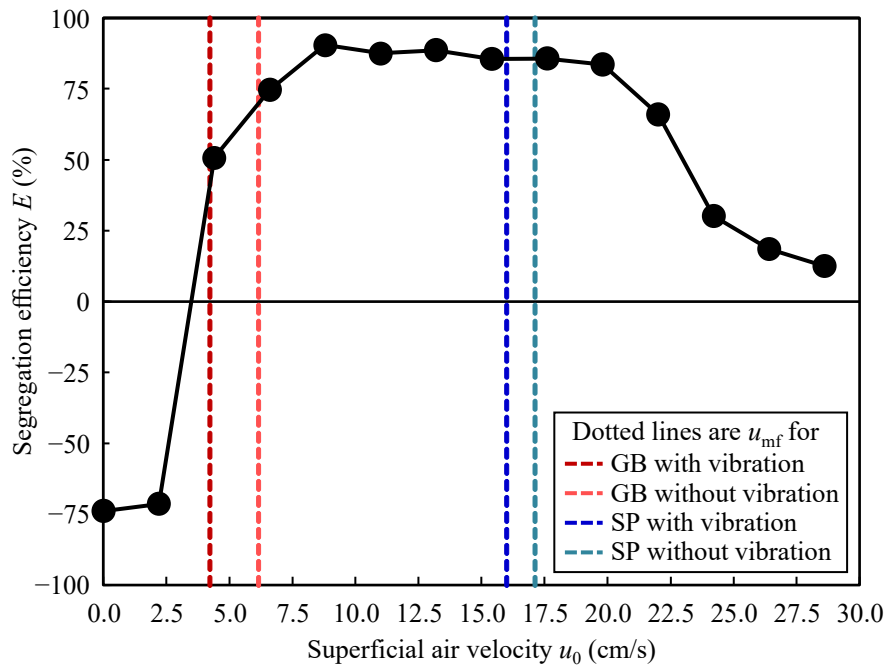


**Fig. 6.** Segregation efficiency  $E$  as a function of superficial air velocities  $u_0$  for Mixture A. Dotted lines are  $u_{mf}$  for each experimental condition.

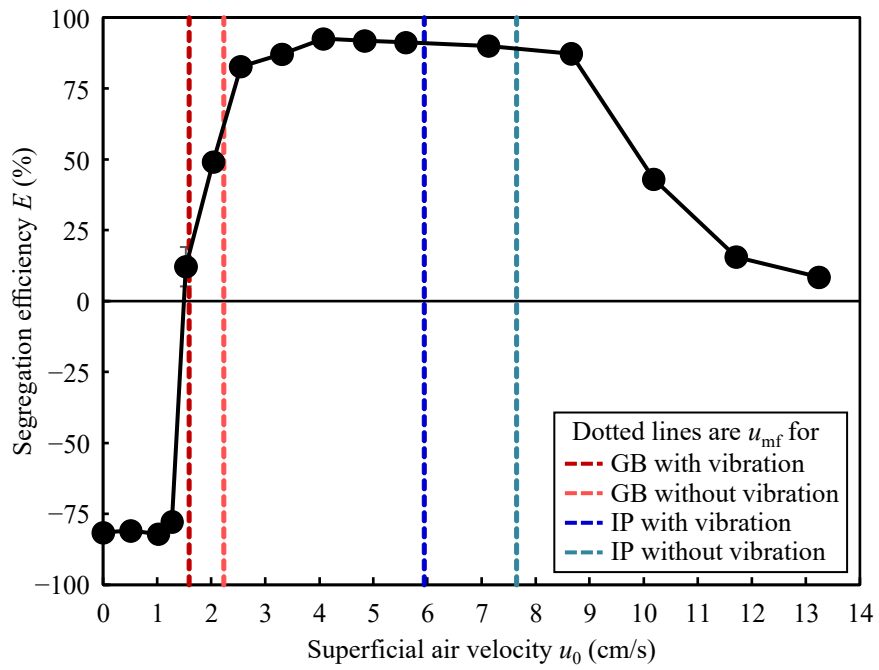


**Fig. 7.** Segregation efficiency  $E$  as a function of superficial air velocities  $u_0$  for Mixture B. Dotted lines are  $u_{mf}$  for each experimental condition.